Characterization of electrochemical systems using Potential Step Voltammetry. Part II: Modeling of Reversible Systems.

A. Martínez-Ibernón[1], J.E. Ramón[1], J.M. Gandía-Romero[1,2], I. Gasch[1], M. Valcuende[2], M. Alcañiz[1,3] and J. Soto[1].

[1]Interuniversity Research Institute for Molecular Recognition and Technological Development (IDM), Universitat Politècnica de València, Universitat de València. Spain
[2]Department of Architectural Construction. Universitat Politècnica de València. Spain
[3]Department of Electronic Engineering. Universitat Politècnica de València. Spain

Abstract

This study was carried out to compare the results obtained using potential step voltammetry and linear sweep voltammetry with a rotating gold disc electrode (RDE), when models based on equivalent circuits (EC) were used. The results lead to an equivalent circuit model that allows us to interpret the electrochemical behavior of aqueous solutions containing $Fe(CN)_6^{-4}$ and $Fe(CN)_6^{-3}$. With this model, we determined the values of the electrical resistance of the medium (R_s) as well as its polarization resistance (R_p), and established correlations between these values and the kinetic parameters of the system. The proposal highlights the need to introduce a new component for modeling using EC, which we have called the electrochemical diode.

Key words: *equivalent circuits, electrochemical diodes, polarization resistance.*

1. Introduction

The application of linear sweep voltammetry to a rotating electrode in a reversible electrochemical system was first modeled theoretically more than 60 years ago [1], [2], [3], and therefore can be considered an electrochemical technique of reference.

On the other hand, although potential step voltammetry has not reached the same levels in its theoretical development, it has become a widely used tool. For example, it is employed as a measurement technique for voltammetric electronic tongues. There are many reasons that have led to its use in this field, including the fact that it is a rapid measurement technique, requires very little maintenance, and consumes little reagent when working with electrodes made of noble metals. In addition, potential step voltammetry can be considered non-destructive [4] and can be easily implemented in routine control applications [5]. Recently, this technique was applied to evaluate the speed of corrosion in reinforced concrete structures, although without much success because the system was inadequately modeled and the analysis of the information collected was excessively simplified [6], [7]. In spite of this, the possibility of automating the monitoring of pathologies in reinforced concrete structures and of their evolution over time is one of the reasons the application of this technique is very attractive in the field of construction.

One of our objectives, as we have indicated in previous papers, is to further explore the modeling of electrochemical processes using equivalent circuits [8], [9]. The purpose is to try to establish relationships that are useful for systematizing and simplifying the analysis of the behavior of electrochemical systems. With the

relationships obtained, the set of data collected during the potential sweep (intensity-time) can then be reduced, condensing it into a small matrix of characteristic parameters. Reducing the dimensions of the information matrix can be especially useful in the field of electronic tongues and noses, since it speeds up the statistical calculations used in principal component analysis (PCA), partial least squares (PLS), and neural network methods [10].

The second objective of this research is to use the potential step technique to establish relationships between the different electrochemical variables and parameters controlling the kinetics of electrode processes (such as the number of electrons (n), the diffusion coefficient (D), the rotation speed of the working electrode (ω), the concentration (C), etc.), and in turn compare those with the values obtained for each of the different resistive or capacitive components (which are found in the equivalent circuits used for modeling).

Thirdly, the aim is to evaluate the coherence of the results obtained using the electrochemical techniques of potential step voltammetry and linear sweep voltammetry.

Finally, we endeavor to establish protocols for the use of equivalent circuits, so that they are conceptually coherent with the type of system studied.

The results and conclusions obtained can be useful in very different areas, such as those related to electronic tongue (ET) technology applied in quality control, and those dedicated to the study of metal corrosion, especially in the area of reinforced concrete structure durability, where the use of equivalent circuits for process modeling is widespread [11] but not very systematized.

3

2. Experimental

The electrochemical tests were carried out with solutions containing Hexacyanoferrate (II) and Hexacyanoferrate (III), one solution with KNO_3 as the background salt and one without. The solvent used was distilled water, which was purified before its use with a Milli-Q system. Working concentrations were 0.1 m for the iron complexes and 0.5 m for KNO_3.

The electrochemical study was carried out using an Autolab PGSTAT101 device with a three-electrode system. A saturated calomel electrode (SCE) was used as the reference electrode. All measurements were made using polycrystalline gold electrodes. The working electrode (WE) was a rotating disc electrode with a surface area of 0.071 cm^2, and its rotating speed was controlled by the Autolab. In this study, rotation speeds between 0 rpm and 5000 rpm were employed. The surface area of the auxiliary electrode was 1.03 cm^2. Prior to use, the electrodes were polished using sandpaper and abrasives of different granulometry, and then rubbed on a soft cloth with alumina and diamond powder until they were smooth and glossy.

All the tests were carried out under Argon atmosphere, to avoid the presence of oxygen due to its oxidizing nature and the alterations that atmospheric CO_2 can produce on the pH of a solution. Measurements were obtained in a Faraday cage to electrically screen the system studied. The temperature was controlled at 25.0 ± 0.1 ºC using a PolyScience SD07R thermostatic bath.

4

The techniques used were linear sweep voltammetry and potential step voltammetry. The range of potential sweeps used with linear sweep voltammetry was between + 0.8 V for the anodic region and -1.0 V for the cathodic area, with respect to the Open Circuit Potential (OCP) value. The sweep speed used was 20 mVs^{-1}.

For potential step voltammetry, the duration of the potential steps was 600 milliseconds, which was sufficient so that at the end of the pulse, the current that crossed the system was almost zero or reached a practically constant value. The OCP value was accepted as valid when the observed potential drift as a function of time was less than 10 μVs^{-1}.

The determination of the resistance R_u value (see Figure 3) was carried out by means of impedance spectroscopy and potential step voltammetry.

3. Results and discussion

3.1 Analysis of electrochemically reversible systems using linear sweep voltammetry with a rotating disc electrode (RDE).

Figure 1 shows the voltammetric curves obtained for the binary system made up of 0.1 m Fe (II) and Fe (III). The intensity-potential curves were recorded at angular rotation speeds of 500, 1500, 3000 and 5000 rpm. The experimental data of this figure is shown after correcting for the ohmic drop of the system.
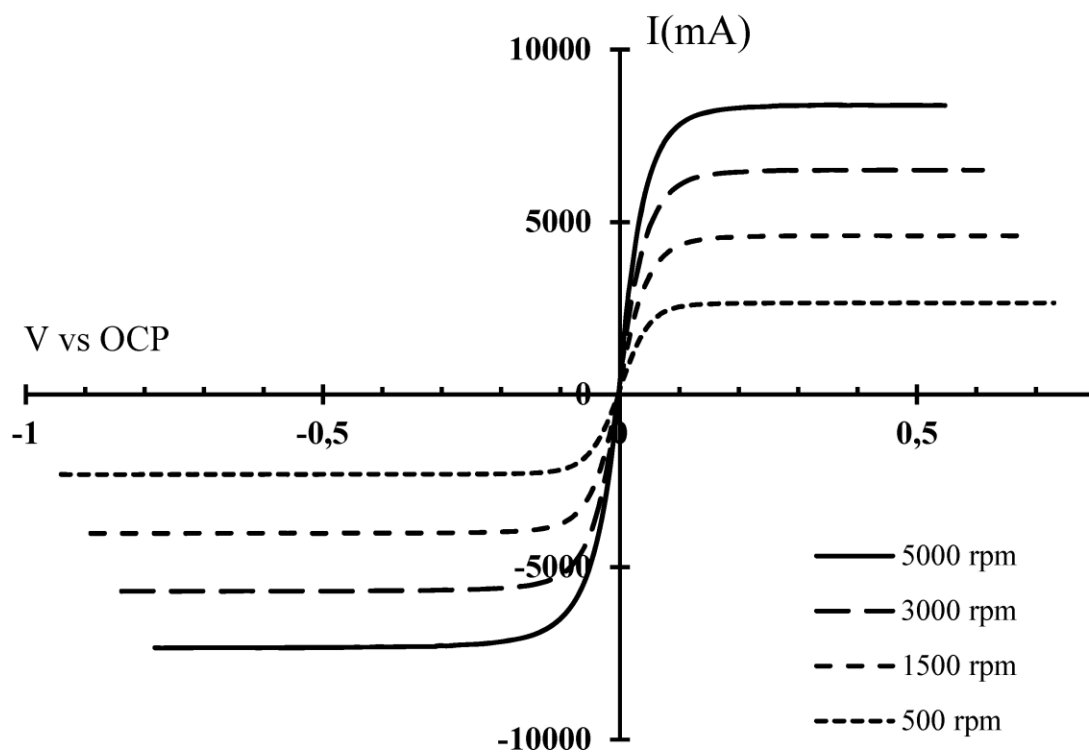
5

Figure 1. Experimental curves of current intensity versus potential with respect to the OCP for the 0.1 m Fe(II)/Fe(III) binary system in aqueous solution.

The electrochemically reversible systems, made up of the redox couple, comply with Eq. 1. This expression relates the net current intensity that passes through the system to the applied potential difference, measured with respect to the value of the half-wave potential of the pair.

$$E = E_{1/2} + \frac{RT}{nF} ln \frac{(i_{Lc} - i)}{(i - i_{La})} \tag{1}$$

6

Where: $E_{1/2}$ = half-wave potential, R = ideal gas constant, T = temperature in Kelvin, n = number of electrons transferred, F = Faraday constant, i_{Lc} = cathodic limiting current, i_{La} = anodic limiting current, I = current intensity for the value of E.

On the other hand, both the anodic and cathodic limiting current intensities of the system must comply with the Levich equation (Eq. 2). This equation indicates that the limiting current intensity of the redox processes (cathodic and anodic) varies linearly with the square root of the rotation speed of the working electrode, which is verified by the experimental data obtained about the system.

$$i_{L(a,c)} = 0.620 \cdot n \cdot F \cdot S \cdot D_{(a,c)}^{2/3} \cdot \omega^{1/2} \cdot v^{-1/6} \cdot C_{(a,c)}^{*} \tag{2}$$

Where: n = number of electrons in the transfer process, F = Faraday's constant, S = surface area of the electrode, $D_{(a,c)}$ = diffusion coefficient of the reduced form (a) or of the oxidized form (c), ω = angular rotation speed of the electrode, v = Kinematic viscosity of the solution, $C_{(a,c)}^{*}$ = concentration in mol/cm^3 of the reduced or oxidized agent.

Taking into account the basic principle of current flow, the total current that circulates through the system must be equal to the sum of the currents transported by the active species in the system. In theory, both the solvent and the complex ions Fe(II) and Fe(III) can act as charge acceptors or charge donors. With this in consideration, Eq. 1 can be used to obtain Eq. 3. The terms $i(E_{ad})$ and $i(E_{cd})$ indicate the anodic and cathodic processes suffered by the solvent.

$$i = \frac{i_{La}}{1 + e^{-\frac{nF}{RT}(E-E_{1/2})}} + \frac{i_{Lc}}{1 + e^{\frac{nF}{RT}(E-E_{1/2})}} + i(E_{ad}) + i(E_{cd}) \tag{3}$$

If the voltammetric sweep is performed in the middle range of the electrochemical window, then the current intensity associated with the redox processes of the solvent is very low and can be disregarded. Under these conditions, the total current intensity can be calculated based on the sum of the current related to the oxidation-reduction of the two iron complexes, so that:

$$i = \frac{i_{La}}{1 + e^{-\frac{nF}{RT}(E-E_{1/2})}} + \frac{i_{Lc}}{1 + e^{\frac{nF}{RT}(E-E_{1/2})}} \tag{4}$$

Table 1 summarizes the values of the limiting current intensities obtained by using Eq. 4 and fitting the current intensity curves against the potential difference (E-$E_{1/2}$). The table shows the information obtained for the 0.1 m Fe(II)/Fe(III) redox couple, with and without 0.5 m KNO_3. The values of the MAPEs (mean absolute percentage errors) corroborate a good fitting of the model.

Table 1 Values calculated using Eq. 4 for sweep data with rotating gold electrode at 25 °C under Argon atmosphere. Legend: i_{La} anodic limiting current, i_{Lc} cathodic limiting current.

rpm	$\omega^{1/2}$ (rad/s)$^{1/2}$	0.1 m Fe(II)/Fe(III)		0.1 m Fe(II)/Fe(III) with 0.5 m KNO_3	
		$i_{La}(\mu A)$	$i_{Lc}(\mu A)$	$i_{La}(\mu A)$	$i_{Lc}(\mu A)$
500	7.24	2648	-2313	2615	-2313
1500	12.53	4538	-4036	4361	-4055

8

3000	17.72	6388	-5709	6236	-5710
5000	22.88	8201	-7302	7850	-7390
	NRMSE	2.12%	0.37%	1.16%	1.02%

Correcting for the ohmic drop was done by fitting the experimental current intensity data against the interfacial potential, taking into account the term I^*R_u, where R_u is the electrical resistance between the Reference and the Working electrodes (see **Figure 2**). The optimized resistance values used to compensate for the ohmic drop in the anodic sweep direction was 20.3±0.5 Ohm for the solution with 0.5 m KNO_3 and 29.6±0.8 Ohm for the solution without the background electrolyte. When the sweep was carried out in the cathodic sweep direction, the values obtained for the two solutions were 20.2±0.8 and 30.2±0.2, respectively. There was a difference of approximately 9.5 Ohm between the system containing only the complex mixture and the solution with background electrolyte. On the other hand, the resistance value for the anodic sweep was approximately the same as for the cathodic scan. Once the ohmic drop of the solution was corrected, the value of the average wave potential was 433 ± 5 mV for the solution without background electrolyte, and 454 ±4 mV (vs. Standard Hydrogen Electrode) for the solution with 0.5 m KNO_3, which is comparable to bibliographic data obtained by other authors for this same system [12].

By applying the slope values of the anodic and cathodic limiting currents vs $\omega^{1/2}$ ($r^2 > 0.998$), we obtained the value of the diffusion coefficient of the oxidized and

9

reduced forms, which were $0.74*10^{-5}$ and $0.64*10^{-5}$ cm^2 s^{-1}, respectively. These results are similar to the values published in other works [13].

3.1.1 Relationship between Rp and the overpotential in equivalent circuits.

In order to model the electrochemical behavior of reversible systems, equivalent circuits such as R_s-(R_p/C) have traditionally been used, like the one shown in **Figure 2**. It shows the values of the voltage drop in a series of points selected between the working electrode (WE), auxiliary electrode (AE), and reference electrode (RE), when in steady state with a current (I) flowing through the system. The difference in total voltage applied between the working electrode and the auxiliary electrode can be referred to as ΔV. On the other hand, the measured potential drop between the working electrode and the reference electrode can be referred to as ΔE_{RW}.
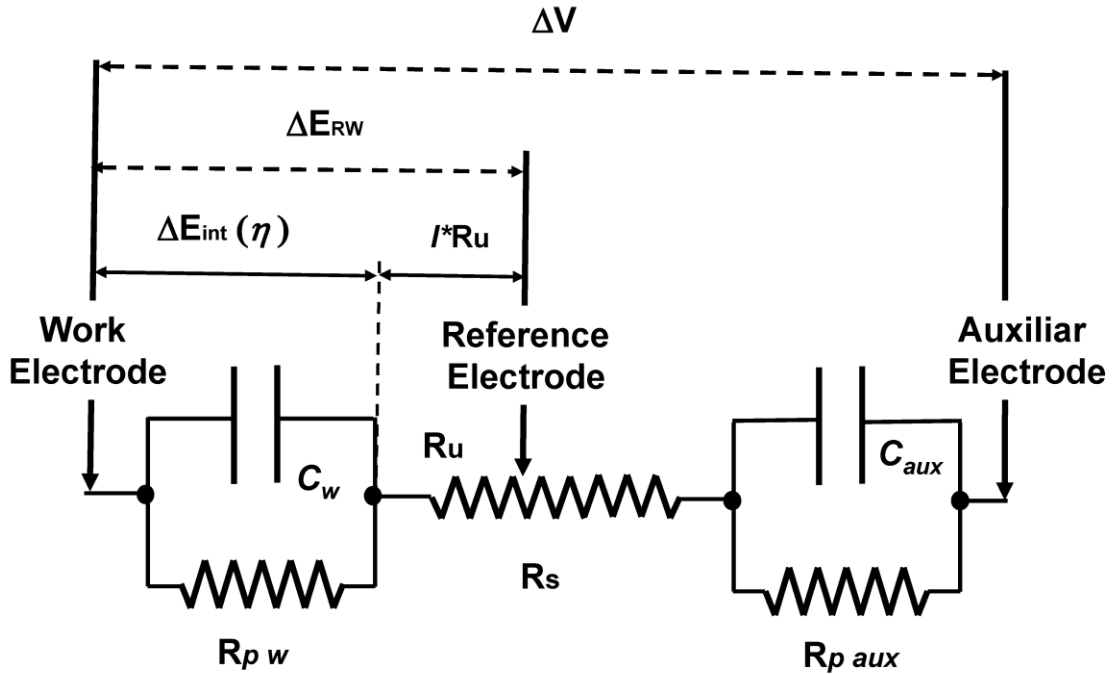
Figure 2. Equivalent circuit used for the study of redox transfer. R_s: Resistance of the solution to ionic circulation. C: Electric double layer capacitor. R_p: Electronic transfer resistance.

This value, as shown in **Figure 2**, must be equal to the sum of the ohmic drop caused by the passage of current (I) through resistor R_u (which is only part of the resistance R_s of the solution) plus the interfacial potential in the electrical double layer (ΔE_{int}), which coincides with the potential drop in the polarization resistance (R_{pw}). If the potential is measured with respect to the OCP value, the ΔE_{int} is the so-called system overpotential η, which in the steady state coincides with the value of I^*R_{pw}. The system overpotential η is defined as the effective interfacial potential measured with respect to the OCP of the system, that is:

$$\eta = \Delta E_{int} - E_{OCP} \tag{5}$$

11

After the correction for the ohmic drop is made, the resistance value R_{pw} is easily calculated by dividing the overpotential by the Faradaic current that passes through the system.

Given that the Faradaic current passing through a reversible system is calculated using Eq. 4, and taking into account that the overpotential is defined as the potential drop in the polarization resistance (R_{pw}), we can apply $I^*R_{pw}=\eta$ to the system and after simplifying, we get Eq. 6:

$$R_{pw} = \frac{\eta}{\dfrac{i_{La}}{1 + e^{-\frac{nF}{RT}(E-E_{1/2})}} + \dfrac{i_{Lc}}{1 + e^{\frac{nF}{RT}(E-E_{1/2})}}} \tag{6}$$

Figure 3 shows the values of R_{pw} for the 0.1 m mixture of Fe(II) and Fe(III) complexes calculated on the basis of the experimental data using Ohm's Law. The values are plotted against the applied overpotential, at different angular rotation speeds (5000, 3000, 1500 and 500 rpm).
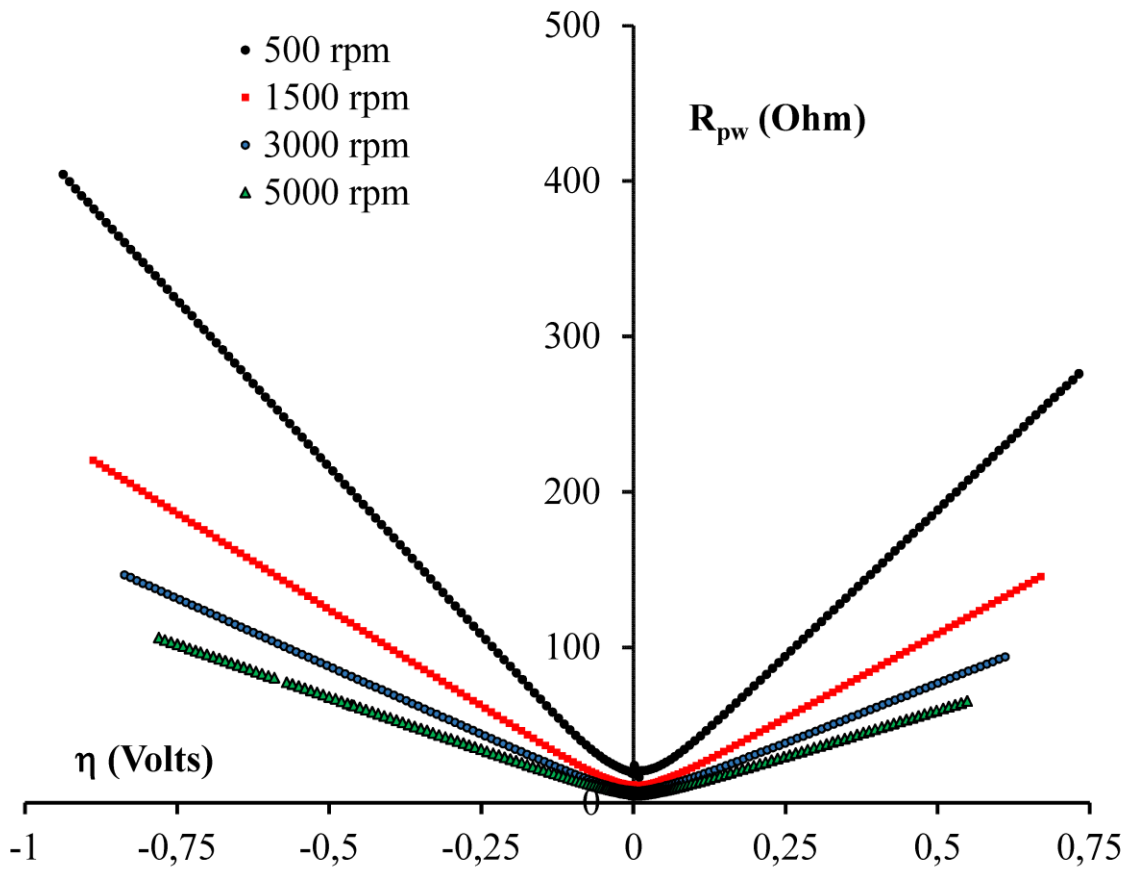
Figure 3. R_{pw} values for the 0.1 m $[Fe(CN)_6]^{-4}/[Fe(CN)_6]^{-3}$ system at rotation speeds of 5000, 3000 1500 and 500 rpm.

The graph reflects a similar shape for each one, with two practically straight stretches on either side of a V-shaped curve in the central region, which corresponds to values close to that of the mean wave potential of the system ($E_{1/2}$). The slopes of the sections that were nearly linear were calculated for each angular rotation speed (R_{pwa}/η for the anodic section and R_{pwc}/η for the cathodic section). Moreover, the theoretical slopes were obtained using Eq. 6. In order to calculate each slope, the term i_{La} was used for R_{pwa}/η and the term i_{Lc} for R_{pwc}/η. The experimental and theoretical data are shown in **Table 2**. The theoretical slope

13

values coincide with the experimental slopes of the almost linear sections, although these values do not correspond to the parallel association of two resistors, for which the slope would be the same for both positive and negative overpotentials. This fact indicates that in order to model the system with equivalent circuits, two R_{pw} resistors in parallel must be added, as well as a discriminating element to control the current flow, so that Eq. 6 is fulfilled.

Table 2. Values of R_{pw} slope for sweep data with rotating gold electrode at 25ºC under Argon atmosphere. Theoretical data: Values obtained through Equation 6. Experimental data: Values obtained through the experimental data.

rpm	$\omega^{1/2}$ (rad/s)$^{1/2}$	0.1 m Fe(II)/Fe(III)				0.1 m Fe(II)/Fe(III), 0.5 m KNO$_3$			
		Experimental data		Theoretical data		Experimental data		Theoretical data	
		R_{pwa}/η	R_{pwc}/η	R_{pwa}/η	R_{pwc}/η	R_{pwa}/η	R_{pwc}/η	R_{pwa}/η	R_{pwc}/η
500	7.24	377	-429	377	-432	384	-425	382	-432
1500	12.53	217	-248	220	-248	223	-246	223	-240
3000	17.72	153	-175	156	-175	158	-174	160	-175
5000	22.88	118	-135	122	-136	124	-136	124	-133
NRMSE				1.23%	0.37%			0.58%	1.81%

The experimental slope values obtained for both dissolutions were very similar (NRMSE: 2.51% for R_{pwa}/η, 0.87% for R_{pwc}/η). This shows that the values of R_{pw} obtained when working in the absence of potassium nitrate coincided with the values obtained when the study was performed in the presence of 0.5 m KNO$_3$. This agrees with the fact that the speed of the oxidation or reduction processes is

not significantly altered by the background electrolyte at the working concentrations used.

Applying limits to Eq. 6, it is easy to verify that when the potential is greater than the half-wave potential, the representation of R_{pw} versus the potential shows an almost rectilinear trend, with slope $1/i_{LA}$. For potentials greater than the OCP, the value of the slope will be the anodic polarization resistance (R_{pwa}), while if the overpotential is cathodic, the function generates a nearly rectilinear section, and from that slope the value of cathodic polarization resistance (R_{pwc}) is obtained.

3.2 Analysis of the system by means of potential step voltammetry. Validation of the method.

In the research that precedes this study, potential step voltammetry has been used to characterize different types of basic equivalent circuits [14]. In this study, we have demonstrated the usefulness of potential step sequences with a design similar to that presented in **Figure 4-A**. This type of pulse pattern is very useful to determine the equivalent circuit model and calculate the values of the different components of the circuit by adjusting the intensity of current or charge with respect to time.

The proposed pulse sequence is formed by a series of steps that are symmetrical with respect to the value of the OCP. The signal pattern shown in **Figure 4-A** has been given the sequence name 0A0C0, where 0 represents the value of OCP, A is the value of the excitation potential of the anodic step, and C the excitation potential value of the cathodic step. The steps returning to the OCP are considered

15

relaxation steps. Another type of equivalent step sequence, which we have called 0C0A0, is characterized by being the inverse of the one shown in the figure.
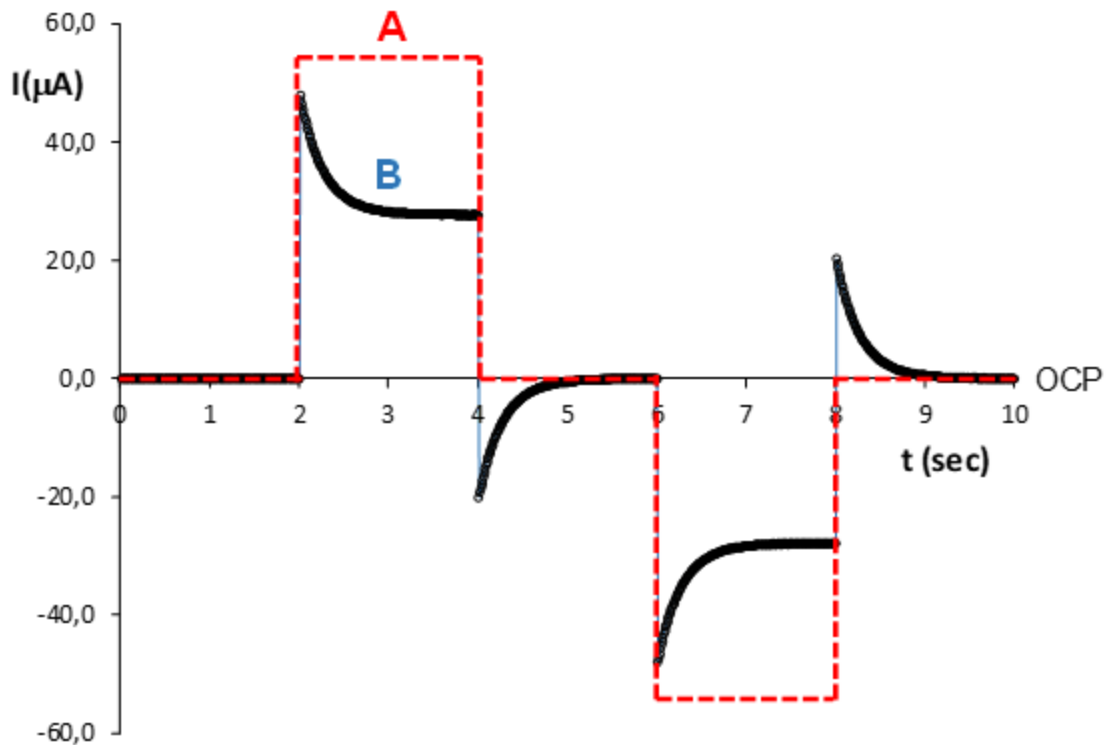

Figure 4. Pulse voltammetry signals. (A) Pulse pattern of potential step voltammetry (0 mV/+300 mV/0 mV/-300 mV/0 mV). (B) Experimental current Intensity for the equivalent circuit Rs-Rp/C with a potential step of 300 mV and the following components: Rs=6200 Ohm, Rp=4700 Ohm and C=95µF

To demonstrate, **Figure 4- B** shows the response of a reduced circuit (R_s-R_p/C) to a sequence of voltammetric steps like those from **Figure 4-A**. The values of R_p and R_s are easily determined based on peak and limiting current intensities reached at the end of each potential step, or based on the corresponding

16

theoretical models. On the other hand, the shape of the current decay, which depends on the time constant (R_s*C), allows us to determine the capacity value (*C*). Finally, it is important to note that when a complete cycle of pulses is carried out with this type of symmetric pulse pattern, the total electric charge accumulated in the system is practically zero.

Figure 5 shows the current intensity response as a function of time when the sequence of pulses shown in **Figure 4-B** is applied for 0A0C0 (solid line) and for 0C0A0 (dashed line), with a potential step of 200 mV and with the disc electrode rotating at speeds of 500, 1500, 3000 and 5000 rpm.
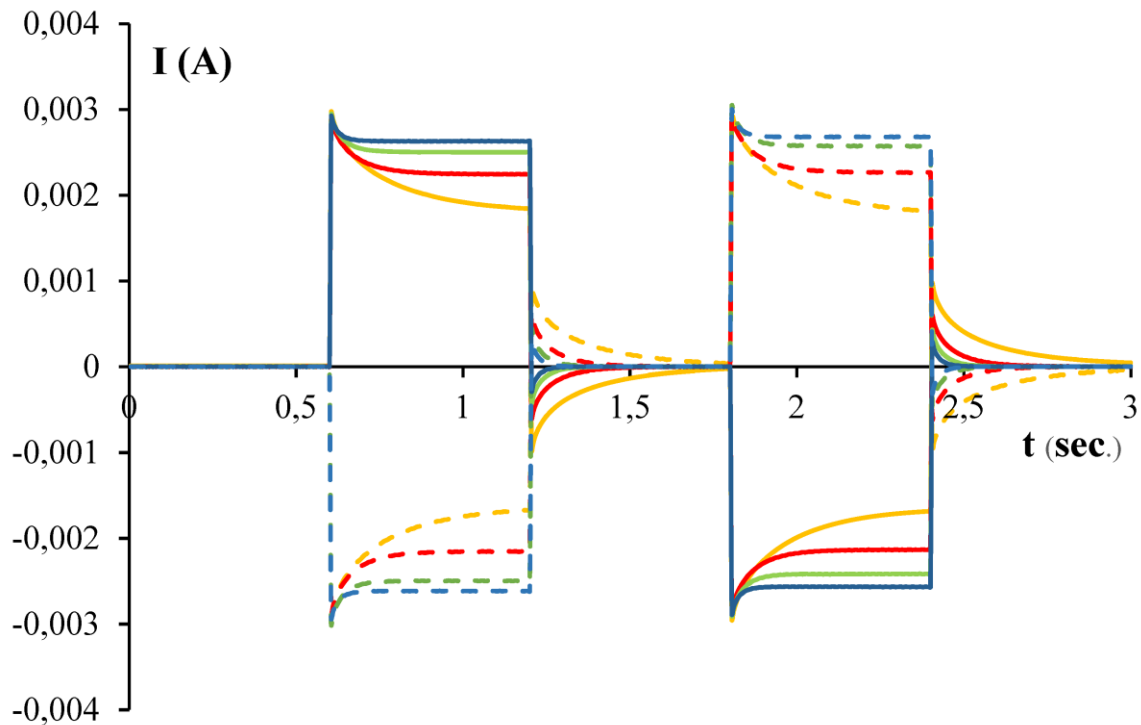
Figure 5. Experimental data for the intensity/time pulses of the 0.1 m Fe(II)/Fe(III) system at different angular speeds of rotation and potential step of 150mV. Solid lines: pulses for 0A0C0. Dashed lines: pulses for 0C0A0. Blue: 5000 rpm, green: 3000 rpm, red: 1500 rpm, and orange: 500 rpm.

The results obtained show two facets that deserve to be highlighted. The first is that the intensity/time behavior is apparently symmetric, regardless of the direction in which the pulse train is applied (0A0C0 or 0C0A0).

The second is that the peak current intensity obtained at the beginning of each step appears to be independent of the angular rotation speed of the electrode. For practical purposes, we can say that the peak intensity associated with the non-Faradaic process only depends on the conductive resistance of the system.

That said, the value of the peak current intensity at the beginning of each pulse allows us to calculate the R_u value of the system, while the value of the current or the limiting charge obtained at the end of the pulse allows us to obtain the value of R_u+R_p. Subtracting the value of Ru from the sum R_u+R_p, we can obtain the value of the resistor Rpw.

The R_u results obtained show a small variation that is dependent on the potential and the rotation speed of the electrode. The mean values of R_u for an overpotential of zero volts are 30.7 ± 0.7 Ohm for the 0.1 m Fe(II)/Fe(III) solution and 20.5 ± 0.8 Ohm for the solution that also contains 0.5 m KNO_3 background salt.

When comparing the Ru values obtained using linear sweep voltammetry and impedance spectroscopy with those calculated using potential steps, a slight difference is observed. Thus, for the solutions of 0.1 m Fe(II)/Fe(III), 30 Ohm (LSV) are obtained compared to 30.7 Ohm (pulses), whereas when working in the presence of 0.5 m KNO_3, values of 20 Ohm are obtained versus 20.5 Ohm, respectively. The difference may be due to the fact that in the second method, the resistance was calculated by extrapolation of the current intensity at time zero of the pulse.

Figure 6 shows R_{pw} values, taking into account the data obtained for different angular speeds of rotation and with different magnitudes for the potential step applied in the sequence 0A0C0. The overpotential values η are calculated by subtracting the ohmic drop value $I*R_u$ from the ΔE_{RW} value.

The results seem to fit two straight lines that form a V, with its vertex centered at the OCP value of the system. The slopes of the two linear branches are different (**Table 3**).

On the other hand, in **Figure 6** the solid line shows the evolution of R_{pw} versus the overpotential for the 0.1 m $Fe(CN)_6^{-4}/Fe(CN)_6^{-3}$ system, with and without potassium nitrate, calculated from the results obtained using linear sweep voltammetry at 1500 and 5000 rpm.
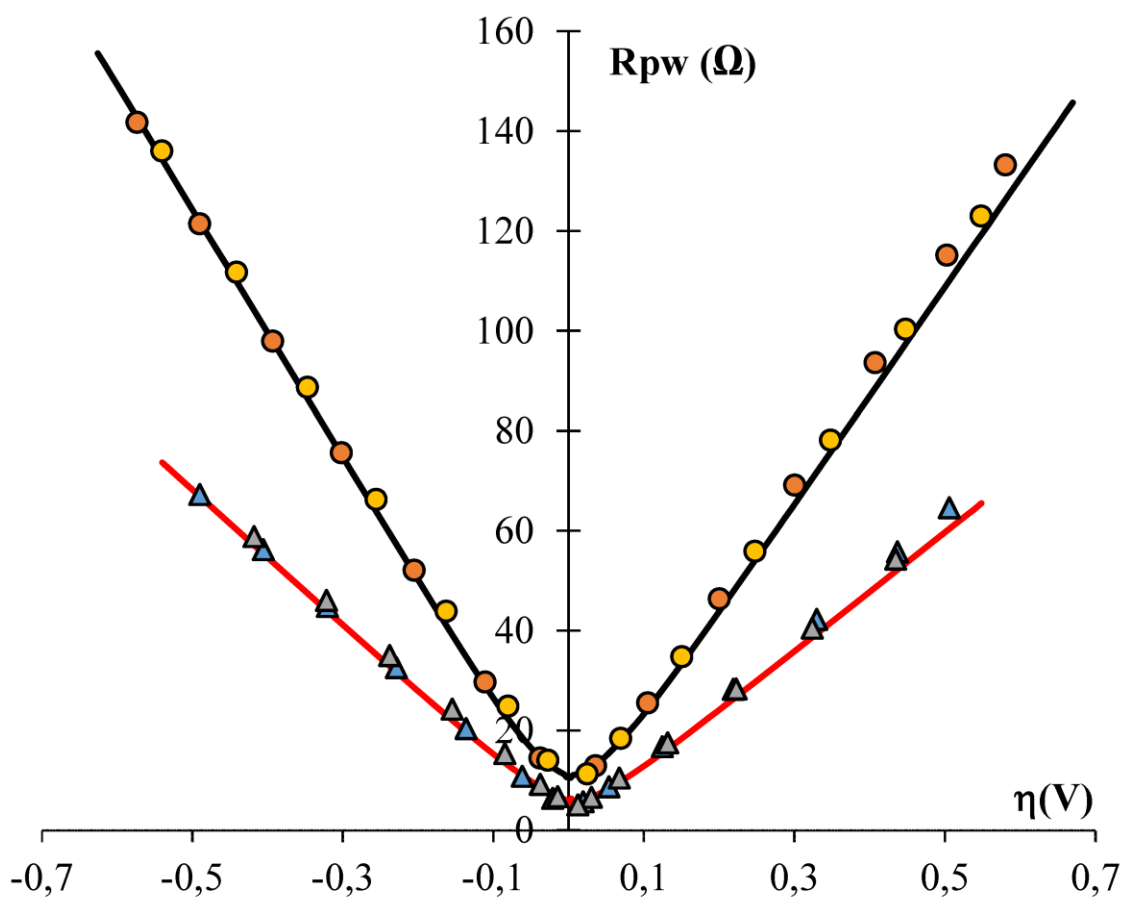

Figure 6. R_{pw} calculated at 1500 and 5000 rpm for the 0.1 m $Fe(CN)_6^{-4}/Fe(CN)_6^{-3}$ system with and without 0.5 m KNO_3 as a background salt. Solid line: linear sweep voltammetry tests with RDE at 5000 rpm(red) and 1500 rpm(black). Colored dots: potential step voltammetry tests.

Table 3 Values of R_{pw} slopes for LSV and potential step voltammetry data with rotating gold electrode at 25ºC under Argon atmosphere. Pulses: Values obtained using potential step voltammetry. LSV: Values obtained using linear sweep voltammetry.

rpm	$\omega^{1/2}$ (rad/s)$^{1/2}$	0.1 m Fe(II)/Fe(III)				0.1 m Fe(II)/Fe(III), 0.5 m KNO3			
		Pulses		LSV		Pulses		LSV	
		$Rpwa/\eta$	$Rpwc/\eta$	$Rpwa/\eta$	$Rpwc/\eta$	$Rpwa/\eta$	$Rpwc/\eta$	$Rpwa/\eta$	$Rpwc/\eta$
1500	12.53	215	-239	217	-247	223	-239	223	-246
5000	22.88	117	-129	118	-135	122	-131	124	-136
NRMSE				0.91%	3.55%			0.78%	3.06%

The overlap of R_{pw} values shown in **Figure 6** validate the results obtained using potential step voltammetry, since they coincide, within acceptable error margins (**Table 3**), with the values obtained using LSV. It is interesting to note that this result opens up the possibility to apply the potential step technique in systems in which linear potential sweep techniques present problems.

3.2.1 Integrated Charge Graph from the potential step scan.

Figure 7 shows the cumulative charge as a function of time, which was calculated from the intensity-time curves corresponding to the pulse voltammetry tests for 0A0C0 (solid lines) and 0C0A0 (dashed lines). The results obtained confirm the conclusions drawn from the current curves in **Figure 6**.
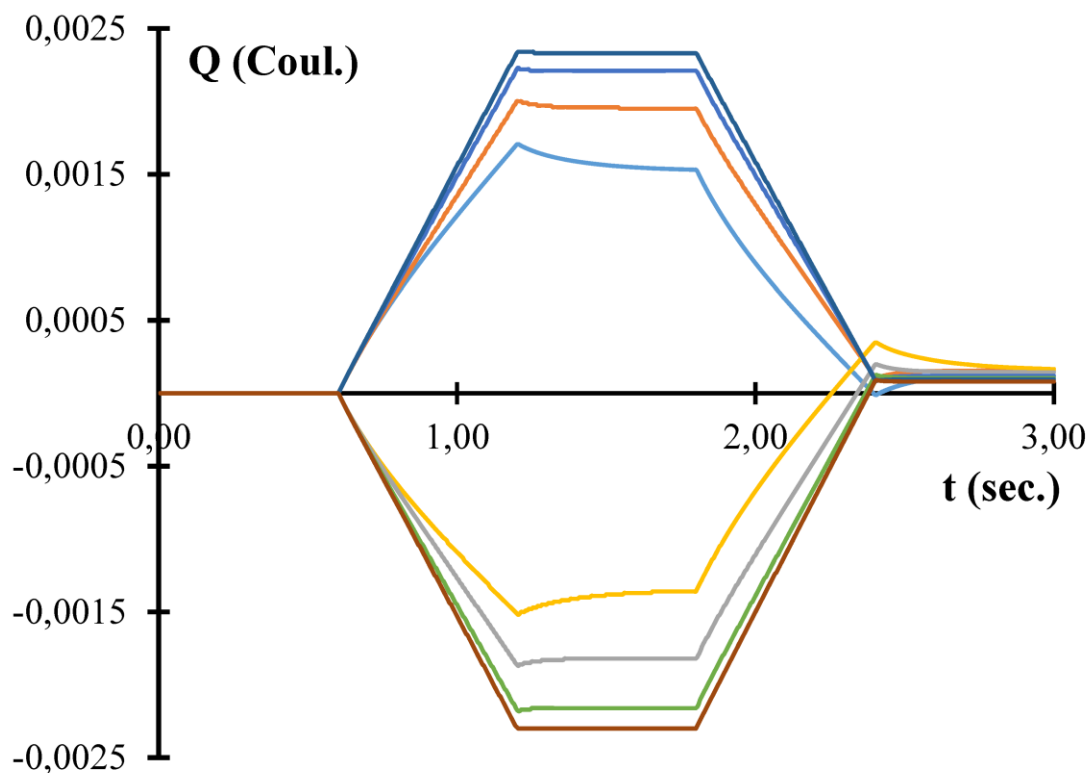
21

Figure 7. Charge/time curves for the 0.1 m Fe(II)/Fe(III) system applying a sequence of AC pulses and its inverse, CA. Solid lines are 0A0C0 pulses. Dashed lines are 0C0A0 pulses. Blue: 5000 rpm, green: 3000 rpm, red: 1500 rpm, yellow: 500 rpm.

Figure 7 shows two interesting aspects. The first is that it clearly demonstrates the relatively small value of the capacitive charge transfer at the interface, compared to the Faradaic charge transfer. In fact, starting from an angular speed of 1500 rpm, the section corresponding to the first charging period (from 0.6 s to 1.2 s) is clearly linear in character. Then, during the relaxation pulse (from 1.2 to 1.8 seconds), non-Faradaic discharge of the double electric layer occurs. This section shows a small peak at the beginning associated with the capacitive discharge and

22

a later horizontal section. For example, at 3000 rpm, the non-Faradaic discharge only represents 3.2% of the total charge transferred at the end of the anodic excitation step.

The second interesting aspect is that the net charge after running a complete cycle of pulses does not return to zero. For the system studied, the total charge transferred during the anodic pulse was greater than the charge transferred during the cathodic pulse, so that under the imposed working conditions, at the end of the potential step cycle there was a net difference of 250 µCoulombs between the anodic and cathodic charge transferred. This is consistent with the fact that the R_{pwa} resistance of the anodic process is less than the transfer resistance R_{pwc} for the cathodic process, as mentioned in the previous sections. This does not mean there is a problem with the reversibility of the process, but rather indicates that the oxidation process is kinetically faster than reduction because of the differences, for this specific case, in the diffusion coefficient of the two complexes (Eq. 2).

Figure 8-A shows the cumulative charge curve of the binary system studied as a function of time. Measurements were performed on a gold electrode at an angular rotation speed of 1500 rpm, when potential steps of 250 mV were applied with a pulse duration of 600 ms. On the other hand, **Figure 8-B** shows the charge curve obtained for a physical circuit R_s-(R_p/C) made up of two resistors, R_s (20 Ω) and R_p (50 Ω), and a capacitor (1.5 mF), when the potential step sequence 0A0C0 was applied with a voltage of 250 mV.
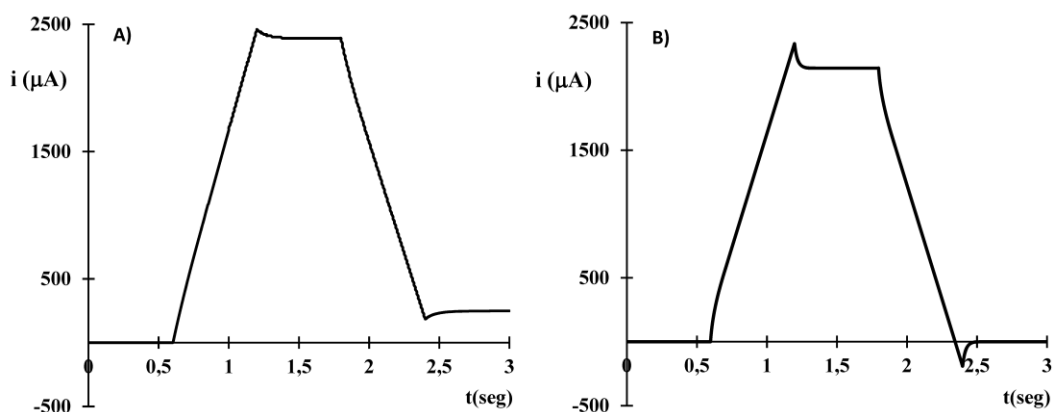
23

Figure 8. (A) Charge-time curve of the Fe(II)/Fe(III) system with Au electrode at 1500 rpm and potential step of 250 mV. (B) Charge curve as a function of time for the equivalent circuit R_s-(R_p/C).

The charge curve presented in **Figure 8-A** shows a shape similar to that shown in **Figure 8-B**, but there is an important difference: the net current charge of Fe(II)/Fe(III) does not return to zero after the full scan cycle is completed. This can be explained by acknowledging that the anodic transfer resistance (R_{pa}) is less than the cathodic transfer resistance (R_{pc}) of the system, as discussed in sections 3 and 3.1. On the other hand, the reversal of the pulse sequence (0C0A0) leads to the same final state of transferred net charge (+250 µCoulomb).

3.3 Equivalent circuit: Modeling of redox processes using electrochemical diodes.

24

For the equivalent circuit to show an electrical response consistent with the described results, it must have the following characteristics:

a) At least two conduction branches arranged in parallel, with the resistor associated with the anodic process (R_{pa}) located in one of the branches and the resistor associated with the cathodic process (R_{pc}) in the other.

b) A current limiting element that controls current flow in each of the branches so that the equivalent resistance of R_{pa} and R_{pc} shows two different values depending on the polarity of the applied pulse (and not an average value).

In electronic circuits, diodes are used to redirect current flow in a specific direction. Electrochemical diodes can be defined analogously as the equivalent circuit elements of an electrochemical cell that determine the direction of the current flow in the anodic and cathodic branches. The analogy between electronic and electrochemical diodes is based on the fact that for both devices the direction of the current flow depends on the sign of the applied potential.

However, some differences can be established between these two elements when forward biased. On one hand, electrochemical diodes present a limitation in the intensity they can carry due to mass transport restrictions. On the other hand, the value of the forward bias voltage for the electronic diodes is always positive and depends on the semiconductor and manufacturing process, while for the electrochemical diode, the forward bias voltage depends on the redox potential of the electroactive species and can be positive or negative. These disparities are easily understood when analyzing the expression of the current flowing through the devices.

25

For the electronic diodes, this expression is given by the Shockley equation (Eq. 7).

$$I = Is \cdot \left(e^{\frac{V}{nVt}} - 1 \right) \qquad (7)$$

Where I is the diode current, I_s is the reverse bias saturation current, V is the voltage across the diode, n is the emission coefficient and Vt is the thermal voltage.

In contrast, Eq. 8 (anodic processes) and Eq. 9 (cathodic processes) give the expression of the current flowing through an electrochemical diode.

$$i_{anod} = \frac{i_{La}}{1 + e^{-\frac{nF}{RT}(E - E_{1/2})}} \qquad (8)$$

$$i_{cath} = \frac{i_{Lc}}{1 + e^{\frac{nF}{RT}(E - E_{1/2})}} \qquad (9)$$

These equations are derived from Eq. 4.

Figure 9 shows a representation of the electrode-solution interface where electrochemical diodes have been included.
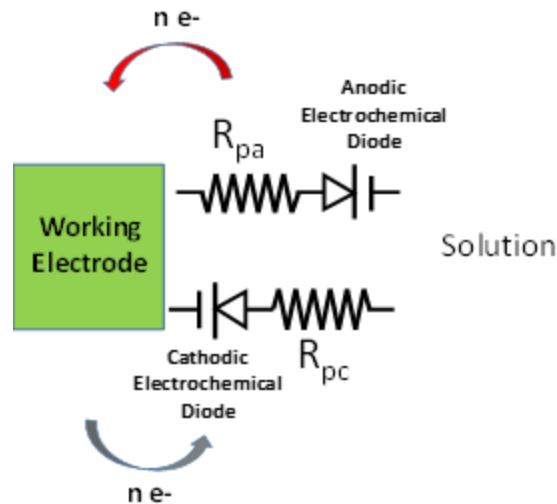
Figure 9 Representation of electrode-solution interface by means of electrochemical diodes.

The electrochemical diode consists of two elements: a battery cell that establishes the forward bias voltage and an ideal diode that allows the current flow in only one direction. In order to include the restrictions to the current imposed by the electrochemical system, a non-linear resistive element (R_p) has been added in **Figure 9**, so that the current flowing through the branch is regulated according to the applied voltage.

Figure 10-A and **Figure 10-B** show the equivalent circuits for anodic and cathodic electrochemical systems. In these diagrams, the effects of the electric double layer and resistance R_s are included. If both diagrams are combined so that the diodes are arranged in opposite directions, a change in the polarity of the applied potential pulse will generate different resistive R_p responses (**Figure 10-C**). Finally, for the model to behave similarly to the experimental one, R_{pa} and R_{pc} have to be accepted

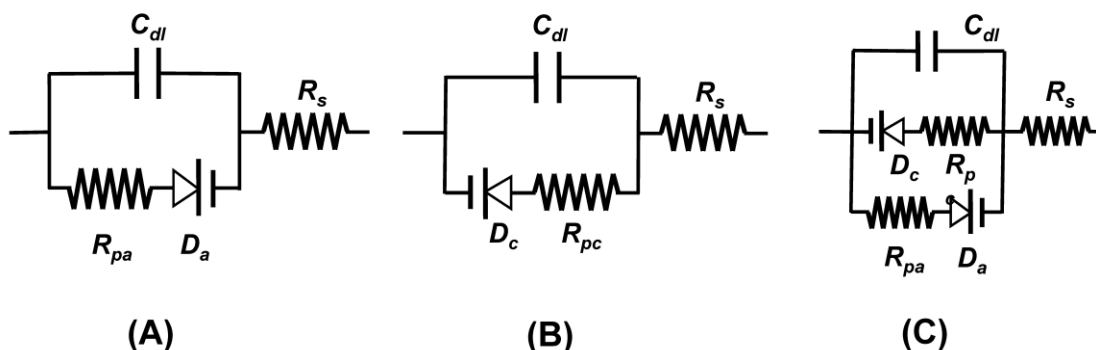as non-linear ohmic resistive devices, whose resistivity depends on the applied overvoltage.

Figure 10. Reduced equivalent circuit with electrochemical diodes. A) Diode in system with oxidation reaction. B) Diode in system with reduction reaction. C) Pair of electrochemical diodes to represent conjugated binary redox systems.

The capacitor C_{dl} was added to emulate the capacitive behavior of the electrode-solution interfacial region. The resistor R_s is necessary in order to take into account the resistive behavior of the electrolytic solution in which the electrodes are located.

A representation that is closer to the actual behavior of an electrochemical cell requires the use of a more complex equivalent circuit than that shown in **Figure 10-C**. In this equivalent circuit, it must be taken into account that electron transfer reactions between the working electrode and the auxiliary electrode are concerted processes. Secondly, any possible transfer processes with respect to the solvent should be considered. Finally, it is necessary to keep in mind that there is a combination of species in contact with the surface of each electrode and, therefore,

28

susceptible to electronic transfer processes. In order to take into account the electrochemical processes of the solvent itself, the proposed equivalent circuit must have at least four branches arranged in parallel. If the solvent transfer potentials vary greatly from those of the system studied, as is the case here, the circuit can be reduced to the diagram shown in **Figure 11**.
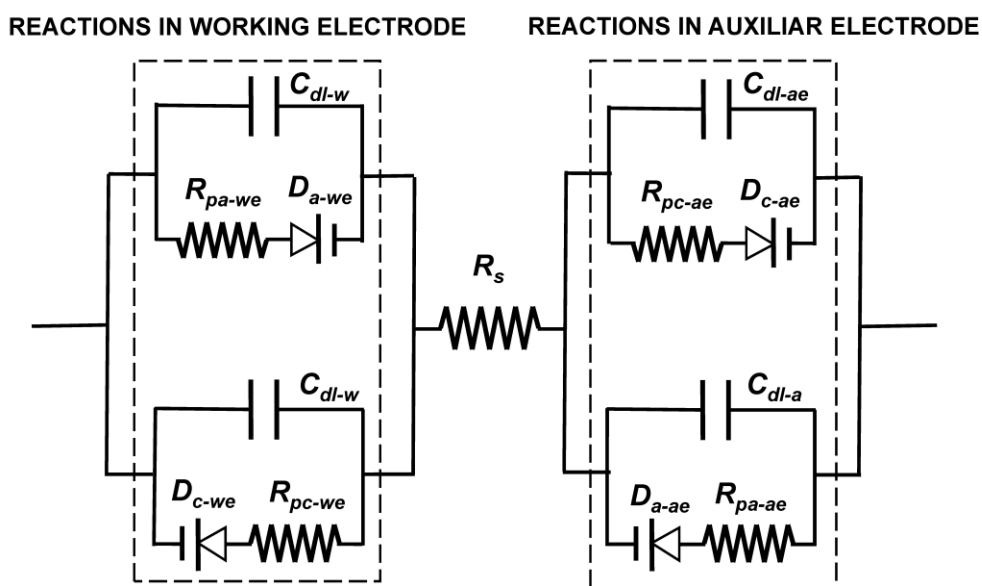

Figure 11. Equivalent circuit formed by a pair of electrochemical diodes. D_a: Diode of the branch associated with the processes during the anodic pulse. D_c: Diode of the branch associated with the processes during the cathodic pulse. R_s: Resistance of the solution to ionic circulation. C_{dl}: double layer Capacity. R_p: Resistance associated with REDOX processes.

Following the requirements mentioned previously, the equivalent circuit has two diodes that act by imposing restrictions on the direction of current flow in each of the two branches where they are located.

When measurements are carried out using the three-electrode technique, the potentiostat controls the voltage difference between the reference electrode and the working electrode, and therefore, for analysis purposes, the circuit shown in **Figure 11** can be reduced to the circuit represented in **Figure 12-A**.
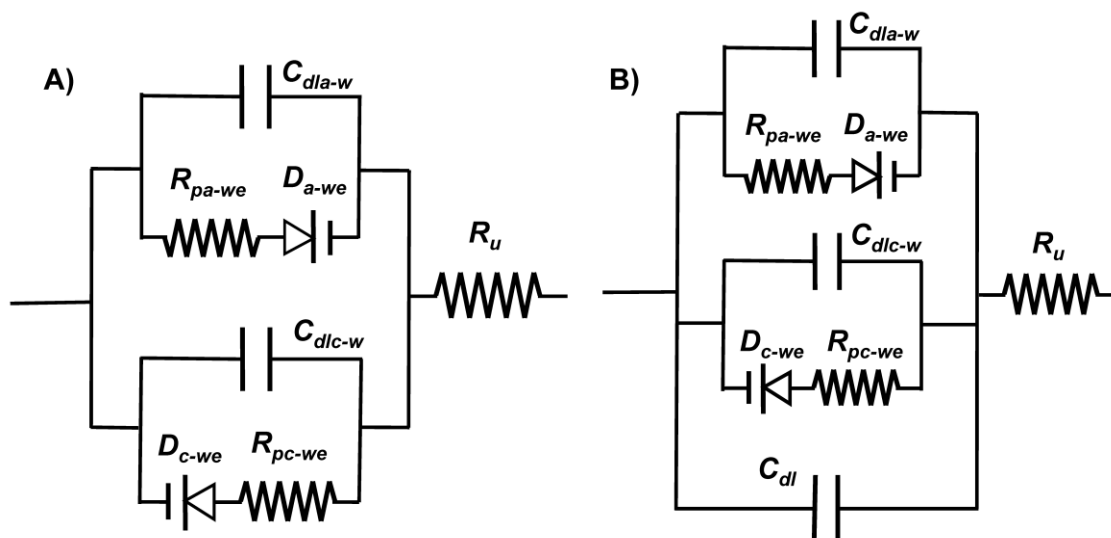

Figure 12. Equivalent circuits when working with three electrodes. D_a: Diode of the branch associated with the processes during the anodic pulse. D_c: Diode of the branch associated with the processes during the cathodic pulse. R_u: Resistance of the solution WE-RE. C_{dl}: Capacity associated with the double layer phenomena. R_p: Resistance associated with REDOX processes. (A) Without background salt. (B) With background salt.

When a background salt such as KNO_3 is used as an inert electrolyte in the solution, it is necessary to add one more branch to the equivalent circuit. In this branch, a capacitor must be included (**Figure 12-B**). This proposal has been verified by optimizing the fitting of experimental data when working with solutions

made up of 0.1 m Hexacyanoferrate (II) and Hexacyanoferrate (III) dissolved with 0.5 m KNO₃, as well as the fitting of data when working with that same binary system in the absence of potassium nitrate.

3.3.1 *Additional verification of the behavior of electrochemical diodes.*

The simplest way to verify the behavior of active redox species such as electrochemical diodes is to carry out a study with solutions made with Fe(II) or Fe(III) species separately.

Figure 13 shows the variation of intensity as a function of time for the pure systems of 0.1 m Hexacyanoferrate (II) (**Figure 13-A**) and 0.1 m Hexacyanoferrate (III) (**Figure 13-B**), obtained when the potential step sequence 0A0C0 is applied, with a step amplitude of 200 mV.
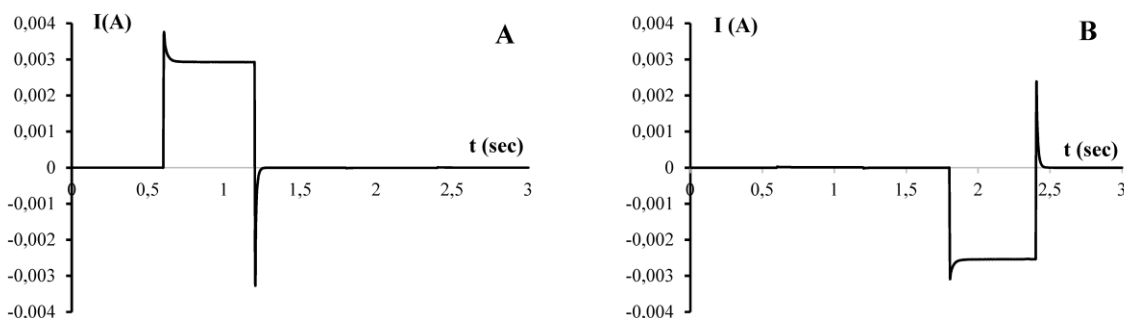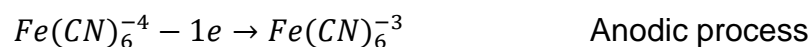

Figure 13. Intensity-time curves. (A) Solution of 0.1 m $K_4Fe(CN)_6$ with Au electrode at 1500 rpm and potential step of 200 mV. (B) Solution of 0.1 m $K_3Fe(CN)_6$ with Au electrode at 1500 rpm and potential step of -200 mV.
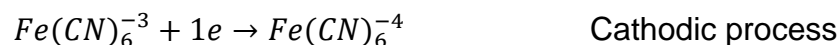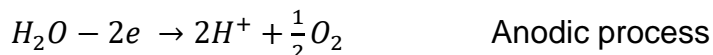
31

Figure 13-A shows significant flow of Faradaic current only in the first anodic excitation step and a second non-Faradaic current peak in its relaxation pulse to OCP. The cathodic excitation step and corresponding cathodic relaxation step show negligible currents. This behavior can be explained by taking into account that the transfer of current at the working electrode occurs when the potential reached is sufficient for oxidation to occur. In view of this, the oxidation of the Fe(II) complex at the working electrode occurs during the anodic pulse. During the cathodic pulse, the process that takes place is the reduction of water. This process occurs in an unfavorable situation due to the low concentration of hydronium ions in the system (pH close to 7) and the small magnitude of the potential step (only -200 mV vs SCE).

$$Fe(CN)_6^{-4} - 1e \rightarrow Fe(CN)_6^{-3} \qquad \text{Anodic process}$$

$$H^+ + 1e \rightarrow \frac{1}{2} H_2 \qquad \text{Cathodic process}$$

Figure 13-B shows the inverse situation to that shown in **Figure 13-A**. In this case, significant flow of Faradaic current is observed only in the cathodic excitation step and the passage of non-Faradaic current in the corresponding relaxation pulse. During the anodic excitation step and the anodic relaxation step there are non-Faradaic currents (two small interfacial charge peaks) and a practically negligible Faradaic current. In this case, the oxidation of the solvent at the working electrode occurs during the anodic pulse. Since the conditions are not favorable for this

32

process to occur due to the low concentration of protons and the insufficient electrical potential applied, the anodic current is negligible. However, when the cathodic pulse is applied, a significant amount of current is observed, associated with the reduction of Fe(III) at the working electrode.

$$H_2O - 2e \rightarrow 2H^+ + \frac{1}{2}O_2 \qquad \text{Anodic process}$$

$$Fe(CN)_6^{-3} + 1e \rightarrow Fe(CN)_6^{-4} \qquad \text{Cathodic process}$$

When potential step voltammetry is applied to binary solutions, the intensity signal obtained is a combination of signals, as shown in **Figure 13**. If the Rpa and Rpc values of the equivalent circuit presented in **Figure 12** are different, the current waveforms for anodic and cathodic pulses will have an asymmetric behavior. This asymmetry is more noticeable for high overpotential values, when one of the diodes is reverse biased and the other is forward biased. If the overpotential value is low, as in electrochemical impedance spectroscopy, the presented equivalent circuit is comparable to traditional models. In this case, none of the diodes are completely reverse biased and the current flows in both anodic and cathodic branches. Therefore, the value of Rp will be a combination of Rpa and Rpc.

This asymmetric behavior of electrochemical systems when large overpotential pulses are applied could explain the discrepancies observed when trying to fit

experimental data obtained with voltammetric electronic tongues to traditional equivalent circuits.

4. Conclusions

Equivalent circuits are used in engineering as a tool to interpret the behavior of complex electrochemical systems. In this study, a series of ideas have been presented that allow us to systematize the proposed design and facilitate its use, while at the same time improve the interpretation of results obtained.

First of all, we established the relationship between the resistance to electron transfer (R_{pwa} and R_{pwc}) and the current intensity, measured using linear sweep voltammetry and a rotating electrode. The experimental results show that it is necessary to employ diodes in the design of equivalent circuits.

Electrochemical diodes act by controlling the direction of current flow, but show important differences in behavior to that of physical diodes, since they do not follow the same physical principles of operation. The Shockley equation, which governs the relationship between intensity and potential for electronic diodes, shows an increasing exponential relationship between the two physical values. The relationship between the intensity and the potential for the electrochemical diode is a sigmoidal function with a limiting current controlled by diffusion as shown in Eq. 3 or Eq. 4. Another difference is the forward bias voltage which, for the electrochemical diode, depends on the redox potential of the electroactive species and can be positive or negative.

34

We also established the theoretical relationship that exists between the variation of R_p and the overpotential when linear sweep voltammetry (LSV) is used on reversible electrochemical systems (Eq. 6). The results show that there is an almost linear dependence of R_p on the overpotential as that value moves away from the OCP of the system.

The R_p values obtained using linear sweep voltammetry (LSV) are the same as those obtained with potential step voltammetry (PSV), a fact that has been considered sufficient to validate the method as well as the procedure proposed to obtain it.

5. Acknowledgements

6. Bibliography

[1] A.J. Bard, L.R. Faulkner, Electrochemical methods : fundamentals and applications, Wiley, 2001. https://www.wiley.com/en-us/Electrochemical+Methods%3A+Fundamentals+and+Applications%2C+

2nd+Edition-p-9780471043720 (accessed November 15, 2018).

[2]   V. Levich, Physicochemical hydrodynamics., Prentice-Hall, Englewood

        Cliffs N.J., 1962. http://www.worldcat.org/title/physicochemical-

        hydrodynamics/oclc/1378432 (accessed November 15, 2018).

[3]   R. Adams, Electrochemistry at solid electrodes, Marcel Dekker Inc, New

        York, 1969. http://www.worldcat.org/title/electrochemistry-at-solid-

        electrodes/oclc/895420950?referer=di&ht=edition (accessed November 15,

        2018).

[4]   C. Krantz-Rülcker, M. Stenberg, F. Winquist, I. Lundström, Electronic

        tongues for environmental monitoring based on sensor arrays and pattern

        recognition: a review, Anal. Chim. Acta. 426 (2001) 217–226.

        doi:10.1016/S0003-2670(00)00873-4.

[5]   P. Ivarsson, M. Johansson, N.-E. Höjer, C. Krantz-Rülcker, F. Winquist, I.

        Lundström, Supervision of rinses in a washing machine by a voltammetric

        electronic tongue, Sensors Actuators B Chem. 108 (2005) 851–857.

        doi:10.1016/J.SNB.2004.12.088.

[6]   G.K. Glass, C.L. Page, N.R. Short, J.-Z. Zhang, The analysis of

        potentiostatic transients applied to the corrosion of steel in concrete,

        Corros. Sci. 39 (1997) 1657–1663. doi:10.1016/S0010-938X(97)00071-1.

[7]   A. Poursaee, Potentiostatic transient technique, a simple approach to

        estimate the corrosion current density and Stern–Geary constant of

reinforcing steel in concrete, Cem. Concr. Res. 40 (2010) 1451–1458.
doi:10.1016/J.CEMCONRES.2010.04.006.

[8]   I. Campos, M. Alcañiz, R. Masot, J. Soto, R. Martínez-Máñez, J.-L.
Vivancos, L. Gil, A method of pulse array design for voltammetric electronic
tongues, Sensors Actuators B Chem. 161 (2012) 556–563.
doi:10.1016/J.SNB.2011.10.075.

[9]   R. Bataller, J.M. Gandía, E. García-Breijo, M. Alcañiz, J. Soto, A study of
the importance of the cell geometry in non-Faradaic systems. A new
definition of the cell constant for conductivity measurement, Electrochim.
Acta. 153 (2015) 263–272. doi:10.1016/j.electacta.2014.12.014.

[10]   A.K. Deisingh, D.C. Stone, M. Thompson, Applications of electronic noses
and tongues in food analysis, Int. J. Food Sci. Technol. 39 (2004) 587–604.
doi:10.1111/j.1365-2621.2004.00821.x.

[11]   E. Barsoukov, J.R. Macdonald, Impedance Spectroscopy: Theory,
Experiment, and Applications, John Wiley & Sons, Inc., Hoboken, NJ, USA,
2005. doi:10.1002/0471716243.

[12]   I.M. Kolthoff, W.J. Tomsicek, The Oxidation Potential of the System
Potassium Ferrocyanide–Potassium Ferricyanide at Various Ionic
Strengths, J. Phys. Chem. 39 (1934) 945–954. doi:10.1021/j150367a004.

[13]   S.J. Konopka, B. McDuffie, Diffusion coefficients of ferri- and ferrocyanide
ions in aqueous media, using twin-electrode thin-layer electrochemistry,

37

Anal. Chem. 42 (1970) 1741–1746. doi:10.1021/ac50160a042.

[14] J.E. Ramón Zamora, A. Martínez, J.M. Gandía, R. Fraile, R.Bataller ,M. Alcañiz, E.García-Breijo and J. Soto. Characterization of electrochemical systems using Potential Step Voltammetry. Part I: Modeling by means of Equivalent Circuits.